Dependency of near-field ground motions on the structural maturity of the ruptured faults

M. Radiguet[1], F. Cotton[1], I. Manighetti[1], M. Campillo[1], J. Douglas [2]

[1] Laboratoire de Géophysique Interne et Tectonophysique, CNRS, Observatoire de Grenoble, Université J. Fourier, LGIT, Maison des Géosciences, BP 53, 38041 Grenoble Cedex 9, France

[2] BRGM - ARN/RIS, 3 avenue C. Guillemin, BP 36009, 45060 Orleans Cedex 2, France

Abstract

Little work has been undertaken to examine the role of specific long-term fault properties on earthquake ground motions. Here, we empirically examine the influence of the structural maturity of faults on the strong ground motions generated by the rupture of these faults, and we compare the influence of fault maturity to that of other source properties (slip mode, and blind versus surface-rupturing). We analyze the near-field ground motions recorded at rock sites for 28 large (M_w 5.6-7.8) crustal earthquakes of various slip modes. The structural maturity of the faults broken by those earthquakes is classified into three classes (mature, intermediate and immature) based on the combined knowledge of the age, slip rate, cumulative slip and length of the faults. We compare the recorded ground motions to the empirical prediction equation of Boore et al. (1997). At all frequencies, earthquakes on immature faults produce ground motions 1.5 times larger than those generated by earthquakes on mature faults. The fault maturity appears to be associated with larger differences in ground motions amplitude than the style of faulting (factor of 1.35 between reverse and strike-slip earthquakes) and the surface rupture occurrence (factor of 1.2 between blind and surface rupturing earthquakes). However the slip mode and the fault maturity are dependent parameters, and we suggest that the effect of slip mode may only be apparent, actually resulting from the maturity control. We conclude that the structural maturity of faults is an important parameter that should be considered in seismic hazard assessment.

Introduction

The level and variability in earthquake ground motions depend on three main factors: the earthquake source properties, the details of the wave propagation through the heterogeneous transmission medium, and the local site effects (e.g., Mai, 2008; Douglas, 2003). While many studies have been conducted in the last couple of decades to quantify the role of local site effects and to improve our understanding of wave propagation, little work has been done to examine which source properties, other than the earthquake size, may have a strong effect on the ground motions. The only 'additional' source properties which have so far been included in ground motion studies are the earthquake slip mode (normal, reverse, or strike-slip; e.g. Bommer et al., 2003), the regional tectonic setting (e.g. Spudich et al., 1999), and the presence or lack of significant coseismic slip at surface (e.g. Somerville, 2003; Kagawa et al., 2004). On the other hand, several studies have suggested that some of the earthquake source properties strongly depend on some of the intrinsic properties of the long-term faults on which the earthquakes occur. The plate tectonic context (intra- versus inter-plate faults; e.g., Scholz et al., 1986), the long-term slip rate (e.g. Anderson et al., 1996), the geometry (e.g., Stirling et al., 1996), and the 'structural maturity' of the long-term faults (Manighetti et al., 2007) have all been recognized as major fault properties having a significant effect on earthquake variability (i.e., variability in stress drop, slip amplitude, rupture length and magnitude). Because it depends together on the age, slip rate, cumulative slip and length of the faults (Manighetti et al., 2007), hence is an integrated property, the structural maturity may be the fault property to have the largest impact on the earthquake source. Our specific objective is to examine whether the fault structural maturity has an influence on the near-field ground motion variability. If such an influence is demonstrated, it may allow significant improvement of the available ground-motion prediction equations (GMPEs), e.g. Douglas, (2003), mainly by permitting a better discrimination of the factors responsible for the variability of ground motions between earthquakes.

We analyze near-field ground motions recorded at rock sites for 28 large (M_w 5.6-7.8) shallow crustal earthquakes of various slip modes. Meanwhile, we examine the structural maturity of the long-term faults broken by the analyzed earthquakes. Following Manighetti et al. (2007), we assign the faults three different degrees of structural maturity (mature, intermediate, immature), defined from the combined knowledge of the age, slip rate, cumulative slip and length of the long-term faults. We then analyze the ground motions as a function of the fault structural maturity, but also of the earthquake slip mode and of the existence or absence of coseismic slip at surface. The ground motion variations are discussed with respect to the empirical prediction equations of Boore et al. (1997), as these equations were derived for crustal earthquakes in the same range of magnitude as the events that we analyze. Choice of a different GMPE should not have a significant impact on the conclusions drawn.

Data

A large quantity of high quality near-field seismological records of strong earthquakes is now available (e.g. the COSMOS database, http://www.cosmos-eq.org/), making it possible to analyze the ground-motion variability in great detail. We found 28 crustal earthquakes for which near-field seismological records are available (Table 1). Those earthquakes are all shallow (i.e., having broken the first 20 km of the crust), so that the depth dependency of the ground motions may be ignored. Consequently, we do not include any subduction event in our analysis. The 28 selected earthquakes span a magnitude M_w between 5.6 and 7.8, and have various slip modes (13 reverse, 12 strike-slip and 3 normal mechanisms). We do not consider the moderate magnitude earthquakes (M_w<6.5) in our study of surface rupture occurrence, because the lack of surface slip for these earthquakes might be a size effect only. Among the 16 earthquakes of magnitude larger than 6.5, 10 earthquakes have clearly broken the surface and 6 are blind rupture earthquakes. To limit the impact of possible local site effects on the ground-motion variability, we only consider records from rock and stiff soil sites, from stations less than 80 km away from the earthquake source (to reduce the effect of possible differences in attenuation, as discussed in Boore et al., 1997). Our total database contains 375 horizontal strong-motion records (Table 2 in electronic supplement). The source-station distance distribution as a function of magnitude is shown in Figure 1. Note that most of the studied earthquakes occurred in western US, so that the results of this study may preferentially apply for tectonic settings similar to this region.

Then, following the approach proposed by Manighetti et al. (2007), we have examined the structural maturity of the long-term faults ruptured by the 28 selected earthquakes. In the regions where the earthquakes occurred, the long-term active faults are generally well known with the geometry of their surface trace (total length, major segmentation, strike variations and associated secondary fault networks), initiation age, maximum long-term slip rate, and total cumulative displacements generally having been determined. We have thus gathered from the literature all information documenting the total length, initiation age, maximum cumulative displacement and maximum slip rate on the long-term faults under analysis, and used these four long-term parameters (when available) to qualify the structural maturity of the faults (Table 1). This caused us to classify the broken faults into the three classes proposed by Manighetti et al. (2007): 'immature', 'intermediate', and 'mature'. Details on the way those three classes are defined are given in the caption of Table 1. We end up with our fault population including 64% of immature faults, 21% of intermediate-maturity faults, and 15% of mature faults. While defining the maturity of the faults, we note that, because they are young, thus small and not generally having a clear surface expression, the immature faults are often less documented than the mature and 'intermediate' faults (Table 1). In the absence of other clear evidence, we consider that a fault that was unknown before an earthquake is an immature fault. All in all, the immature faults, which basically are young and/or slow-slipping faults, form a population that markedly differs from the long-established and generally well-known intermediate and mature faults. This will make us, at some points of our study, to analyze together the intermediate and mature faults, in comparison to the clearly different population of immature faults.

Analysis

We determine the pseudo-acceleration response spectra of the ground motions in the period range 0.1-2 seconds, and compare them to the empirical ground motions prediction previously proposed by Boore et al. (1997) for non-specified style of faulting. The model of Boore et al. (1997) predicts response spectral pseudo-acceleration as a function of moment magnitude, distance, and site condition. We selected this equation as a reference because it was derived from shallow crustal earthquakes in the same range of magnitude (M_w 5.3-7.7) than the events of our database (M_w 5.6-7.8), and it additionally allows the specification of the site conditions. We set the shear-wave velocity averaged over the upper 30 m of the ground (V_{s30}) to 620 m/sec as suggested by Boore et al. (1997) for generic rock sites.

For each period and station, we determine the residual as the difference between the common logarithm of the response spectra of recorded horizontal motion and the logarithm of the horizontal acceleration predicted using the GMPEs of Boore et al (1997). Figure 2 shows the data analysis separately for earthquakes having occurred on immature (a-c), intermediate-maturity (d) and mature (e) faults. Each line on the a-e plots represents the residuals for one earthquake averaged over all the recording stations. As a large number of earthquakes have occurred on immature faults, for clarity, we discriminate their ground motion records as a function of the number of recording stations. Plots a and b, that include earthquakes recorded at more than 10 and at 3 to 10 stations, respectively, are thus the best constrained. The zero line is where there is no bias with respect to the model of Boore et al. (1997). Lines above the zero reference indicate earthquakes whose ground motions exceed the model predictions. Note that a 0.1 unit of common logarithm equals a factor of nearly 1.26.

In the period range considered, the ground motions generated by earthquakes on immature faults (best constrained plots a and b) generally exceed the model level, while those generated by earthquakes on mature faults (plot e) are systematically lower than the prediction level. The ground motions produced by earthquakes on immature faults are therefore larger than those generated by earthquakes on mature faults. The earthquakes rupturing faults of intermediate maturity (plot d) have ground motions on both sides of the reference level, but most of them (4 out of 6) have motions below this level.

To compare the influence of fault structural maturity with other source parameters, we then classify the recorded ground motions according to: (i) the structural maturity of the long-term ruptured faults, (ii) the faulting mechanism of the earthquakes (reverse and strike-slip categories as defined by Boore et al. (1997); normal events are too few to be analyzed separately), and (iii) the existence or absence of significant surface slip. Because there are few earthquakes on mature faults, and because, as discussed before, ‘intermediate’ and mature faults are in any case far more mature than any immature fault, in the following we analyze together the earthquakes having occurred on 'intermediate' and mature faults. All the parameters eventually assigned to the earthquakes are reported in Table 1.

To examine how the strong motions vary as a function of the parameters defined above, we use two different methods. First, following Kagawa et al. (2004), we average the residuals for all earthquakes pertaining to any of the categories defined above. Figures 3 a-b-c show the averaged residuals as a function of the structural maturity of the broken fault (a), of the slip mode of the earthquakes (b), and of the existence or lack of significant surface break (c). It confirms that motions produced by the rupturing of immature faults are systematically higher by a factor of 1.35 (0.13 units of common logarithm) than motions generated by earthquakes on mature faults. When earthquakes are distinguished by their mechanism, the same order of difference is observed (factor 1.35), with ruptures on reverse faults producing larger strong motions than earthquakes on strike-slip faults. By contrast, we observe a smaller difference (factor of 1.12) in the ground motions produced by blind and surface-breaking earthquakes.

Then following Spudich et al. (1999), we use a more sophisticated method to determine the mean value of the residuals (called the bias) and its standard deviation for each group of earthquakes. This method allows the residuals to be weighted by the number of records. Figures 3 d-e-f confirm the previous observations. As a matter of fact, the ground motions generated by earthquakes on immature faults are systematically higher by a factor of 1.5 (0.18 units of common logarithm) than the ground motions generated by earthquakes on mature faults, at all frequencies. The difference in the weighted mean (bias) between the two categories is increased compared to the case where residuals are not weighted (Figure 3a). The ground motion difference due to the style of faulting is the same as in Figure 3b (unweighted average) with ground motions on reverse faults being 1.35 times higher than those on strike-slip faults. The surface rupture occurrence seems to have less influence on the ground motions, as blind earthquakes apparently generate ground motions 1.2 times higher than surface-breaking earthquakes for periods lower than 1 second (the difference is slightly increased compared to Figure 3c).

When we determine the bias following Spudich et al. (1999) approach (weighted average), a larger difference is observed in the average of residuals on mature versus immature faults, compared to the unweighted study. The ground motion differences due to the fault maturity are thus larger than those due to the style of faulting. Our results also show that the standard deviations associated with the fault maturity classification (Figure 3d) are lower than the standard deviations associated with the other classifications (style of faulting or surface rupture occurrence), where most error bars overlap.

Our results thus suggest that among the parameters studied, the fault structural maturity is the one to have the most influence on ground motions since it generates the largest differences and the lowest standard deviations. The style of faulting also appears to have a significant effect on ground motions. Yet, it is important to note that there is a dependency between the two factors in our data set as 11 out of 13 of the reverse faults are immature while 8 out of 12 of the strike-slip faults are 'intermediate' or mature. To check whether the effect of fault maturity on ground motions is real or apparent, we test the influence of fault maturity on earthquakes having the same style of faulting. Figures 4 a-b show the averaged residuals computed following Kagawa et al. (2004) and Spudich et al. (1999) for strike-slip earthquakes discriminated from the structural maturity of their broken faults. The difference between ground motions on immature and mature faults still appears though it is smaller than before (averaging a factor of 1.18 for the unweighted average and 1.25 for the bias). Going back to the entire earthquake population, we note that the only two reverse earthquakes which have occurred on mature and intermediate faults (1991 Uttarkashi and 1999 Chi-Chi) do not have residuals particularly higher than those of the other earthquakes having broken mature and 'intermediate' faults (Figures 2 d-e). Thus, the low residuals observed for these two earthquakes do no result from the style of faulting only. Together these results make us suggest that the fault structural maturity is likely the parameter accounting for those low residuals.

Our observations thus show that independently of the style of faulting, the fault structural maturity has an influence on the earthquake ground motions. The two parameters are not independent however, and they both affect the earthquakes ground motions. We suggest that the effect on ground motions commonly attributed to the faulting mechanism is only apparent and more likely results from the fault structural maturity control.

Discussion and Conclusions

Since the 1930s when the first strong-motion networks were installed, the ground motion records have been used to derive empirical ground motion prediction equations which describe how ground motions vary as a function of a limited number of independent parameters, namely the earthquake magnitude, the source-site distance, and some site-specific parameters.

Most of the available equations are summarized and compared in the review paper of Douglas (2003). This synthesis highlights that available equations significantly differ from one to the other and that the uncertainties in all equations have not decreased in the last 30 years. The large uncertainties suggest that some of the factors that govern the ground motion variability have not been included in the GMPEs.

Reducing both the aleatory and the epistemic uncertainties that affect the ground motion predictions is thus a key challenge for engineering seismologists. Following Douglas (2003), we suggest that the large intrinsic and epistemic uncertainties partly result from our incomplete understanding of the factors that govern the ground motions variability and that adding more independent parameters to the GMPEs should reduce the ground motions variability. In addition to the path and site effects, the few sources parameters (other than the earthquake size) that have been included in the equations are the earthquake mechanism (normal, reverse, or strike-slip; e.g. Bommer et al., 2003), the regional tectonic setting (commonly defined by the earthquakes' geographical location; e.g. Spudich et al., 1999), the presence or lack of significant coseismic slip at surface (e.g. Somerville, 2003; Kagawa et al., 2004). Recent reviews suggest other parameters that could be included in GMPEs: Douglas (2003) suggests considering the static stress drop, Anderson et al. (2000) the total fault offset.

Though the earthquake static stress drop varies in a narrow range, its variation generates large differences in the radiated energy and displacement produced on the rupture plane (for a given length). It is thus likely that stress drop variations have significant effects on ground motion variability. Recently, it has been shown that the earthquake static stress drop strongly depends on the structural maturity of the broken faults (Manighetti et al., 2007; Choy and Kirby, 2004); faults that have been slipping for long and/or slipping at a fast rate obviously break in lower stress drop earthquakes than young, immature faults (Scholz et al., 1986; Anderson et al., 1996; He et al., 2003). The stress drop difference would result from the strength and friction on the fault plane reducing as the fault accumulates more slip in time (Choy et al., 2006; Choy and Kirby, 2004; Ben-Zion and Sammis, 2003). Manighetti et al. (2007) propose a way through which the structural maturity of the long-term faults can be assessed before those faults break in an earthquake. This offers the possibility of including the fault structural maturity in GMPEs, and to use it as an independent parameter that basically describes the expected earthquake static stress drop.

This is what we have done in the present analysis. Using the criteria proposed by Manighetti et al. (2007), we have determined the degree of structural maturity of the long-term faults broken by the earthquakes under analysis. We have then used the maturity parameter to classify the ground motion records and analyze their behavior separately in each of the maturity classes. The results show (Figure 3a) that, at all frequencies, the ground motions produced by earthquakes having broken immature faults are 1.5 times larger than those generated by earthquakes on mature faults. This suggests that the structural maturity of the long-term faults broken by the earthquakes is an important factor that governs, at least partly, the variability of the near-field strong ground motions. The observed reduction of ground motions with increasing fault maturity is coherent with a lower stress drop for earthquakes on mature faults than on immature faults. These results are also in agreement with the suggestion of Anderson et al. (2000) that the low accelerations recorded during the 1999 Izmit and Chi-Chi earthquakes compared to the 1992 Landers and 1994 Northridge earthquakes may be related to characteristics of the broken fault; they suggest that the low accelerations produced are related to smooth fault traces resulting from large geological offsets.

When earthquakes are distinguished by their faulting mechanism (Figure 3b), we find that

ruptures on reverse faults produce ground motions about 1.35 times larger than earthquakes on strike-slip faults. This result is coherent with the range of 1.2 to 1.4 proposed by Bommer et al (2003) for the ratio of reverse to strike-slip ground motions. The fault maturity thus generates larger difference in the ground motion than the style of faulting. Yet, there is a dependency between the two factors, since most of the mature earthquakes of our data set are strike-slip. This may be due to the fact that strike-slip earthquakes are more likely to extend in length and accumulate large offsets than dip-slip earthquakes, and thus are more likely to become mature faults. When only strike-slip earthquakes are considered (Figure 4), a difference in the strong-motion amplitude (averaging a factor 1.25) is still observed between earthquakes on immature and mature faults. This suggests that the effect on ground motions commonly attributed to the faulting mechanism may only be apparent and more likely result from the fault maturity control.
Finally, our data show smaller differences in the amplitude of ground motions produced by blind and surface-breaking earthquakes, compared to the results of Somerville (2003) and Kagawa et al. (2004), who found ground motions from buried ruptures being 1.8 times larger than motions produced by surface-breaking earthquakes (in the period range around 1 second). Our results show in the same frequency range that ground motions from buried earthquakes are only 1.25 times (~0.09 units of common logarithm) larger than surface-rupturing earthquakes. Because our results arise from an updated denser dataset, which includes only rock and stiff soil sites (contrary to Somerville (2003) and Kagawa et al. (2004) studies), we suggest that our data are less likely to be biased by site effects and that they are better constrained than before, making us conclude that, for large shallow earthquakes ($M \geq 6.5$), the way the rupture terminates upward has little effect on the ground motion variability.

We conclude that the degree of structural maturity of the long-term faults is a factor that likely plays a significant role in the strong ground motions variability; when rupturing in large earthquakes, immature faults obviously produce larger ground motions than would mature faults breaking in a similar magnitude earthquake. The structural maturity of a fault can be assessed a priori and independently of any knowledge of either the past or future earthquakes. It is thus an independent parameter that should be included in the GMPEs, in addition to the common parameters describing the expected earthquake size, wave propagation path, and site characteristics. One simple way to include the effect of fault structural maturity in the available equations is to apply them with an adjustment factor. Provided that the equation chosen for calculation includes no style-of-faulting parameter, we suggest that the equation be lowered by a factor of 0.7 when the earthquake is expected to occur on a mature fault, and be increased by a factor of 1.12 when the earthquake is expected to occur on an immature fault.

Data and Resources

Accelerograms used in this study are available via the COSMOS online database (http://db.cosmos-eq.org). The list of records used is available in the electronic supplements.

Acknowledgments

The work has been done in the framework of a scientific project (QUAKonSCARPS) funded by the French ANR (N° ANR-06-CATT-008-01). John Douglas's contributions to this study were supported by internal BRGM projects. Fabrice Cotton and Michel Campillo benefited from Institut Universitaire de France support. We thank an anonymous reviewer for their useful comments on an earlier version of this article.

References

Anderson, J. G., J. N. Brune, R. Anooshehpoor, and S. D. Ni (2000). New ground motion data and concepts in seismic hazard analysis, *Curr. Sci*. **79**, 1278 –1290.

Anderson, J. G., S. G. Wesnousky, and M. W. Stirling (1996). Earthquake size as a function of fault slip rate*, Bull. Seism. Soc. Am*. **86**, 683–690.

Ben-Zion, Y., and C. G. Sammis (2003). Characterization of fault zones*, Pure Appl. Geophys.* **160**, 677–715.

Bommer, J. J., J. Douglas, and F. O. Strasser (2003). Style-of-faulting in ground-motion prediction equations, *Bull. Earthquake Eng.* **1**, 171–203.

Boore, D. M., Joyner, W. B. (1997). Site amplifications for generic rock sites, *Bull. Seism. Soc. Am*., **87**, 327–341.

Boore, D., W. Joyner, and T. Fumal (1997). Equations for estimating horizontal response spectra and peak acceleration from western North American earthquakes: a summary of recent work, *Seism. Res. Lett.* **68**, 128–153.

Choy, G., A. McGarr, S.H. Kirby and J. Boatwright (2006). An overview of the global variability in radiated energy and apparent stress*, Geophys. Monogr. Ser*, edited by R. Abercrombie, A. McGarr, and G. Di Toro, **170**, 43–57.

Choy, G. L., and S. H. Kirby (2004). Apparent stress, fault maturity and seismic hazard for normal-fault earthquakes at subduction zones, *Geophys. J. Int.* **159**, 991 –1012.

Douglas, J. (2003). Earthquake ground motion estimation using strong-motion records: A review of equations for the estimation of peak ground acceleration and response spectral ordinates. *Earth-Science Reviews* **61**, 43–104.

He, C., T.-F. Wong, and N. M. Beeler (2003). Dynamics of a spring-slider system with rate and state dependent friction: numerical simulations of the effects of loading velocity and recurrence time for two different evolution laws, *J. Geophys. Res*. **108,** no. B1, 2037.

Kagawa, T., K. Irikua, and P. G. Somerville (2004). Differences in ground motion and fault rupture between the surface and buried rupture earthquakes, *Earth Planets Space* **56**, 3–14.

Mai, P.M. (2008). Ground Motion: Complexity and Scaling in the Near Field of Earthquake Ruptures, in *Encyclopedia of Complexity and Systems Science*, W.H.K. Lee and R. Meyers (Editors), Springer. accepted

Manighetti, I., M. Campillo, S. Bouley, and F. Cotton (2007). Earthquake scaling, fault segmentation, and structural maturity, *Earth Planet. Sci. Lett.* **253**, 429–438.

Scholz, C. H., C. Aviles, and S. Wesnousky (1986). Scaling differences between large intraplate and interplate earthquakes, *Bull. Seism. Soc. Am.*, **76**, 65-70.

Somerville, P. G. (2003). Magnitude scaling of the near fault rupture directivity pulse, *Phys. Earth Planet. Interiors* **137,** 201–212.

Spudich, P., W. B. Joyner, A. G. Lindh, D. M. Boore, B. M. Margaris, and J. B. Fletcher (1999). SEA99: a revised ground motion prediction relation for use in extensional tectonic regimes, *Bull. Seism. Soc. Am.* **89**, 1156–1170.

Stirling, M. W., S. G. Wesnousky, and K. Shimazaki (1996). Fault trace complexity, cumulative slip, and the shape of the magnitude-frequency distribution for strike-slip faults: a global survey, *Geophys. J. Int.* **124**, 833-868

Figures

Figure 1. Distribution of recordings in magnitude and distance (Joyner and Boore distance r_{jb}). The data are separated into three classes, depending on the structural maturity of the faults broken by the analyzed earthquakes.

Figure 2. Ratio of response spectral amplitude of individual earthquakes averaged over recording sites to that of the GMPEs of Boore et al. (1997). The zero line represents no bias with respect to the GMPE. The residuals represent the common logarithm of the event/model ratio: +0.1 indicates that the average event ground motion exceeds the model by a factor of 1.26 and -0.1 indicates event ground motion at 0.79 of model value. The number of recording stations for each earthquake is indicated in the legend. (a), (b) and (c) show residuals for earthquakes on immature faults, (d) and (e) show earthquakes on intermediate and mature faults, respectively.

Figure 3. Comparison of the influence of different source factors on the ground motions. (a-b-c) plots show average of residuals (the common logarithm of the event/model ratio) for events following Kagawa et al.'s method; (d-e-f) plots show weighted average of residuals and standard deviation following Spudich et al.'s method. The source parameters considered are fault maturity (a-d), style of faulting (b-e) and existence or absence of surface break (c-f).

Figure 4. Influence of fault maturity with a constant style of faulting (strike-slip). (a) Average of residuals (using approach of Kagawa et al.); (b) Weighted average of residuals (using approach of Spudich et al.).

Table

Table 1. Structural maturity of the long-term faults broken by the analyzed earthquakes, and characteristics of the earthquakes.

L is the long-term fault length in km; I-Age the age of fault initiation in millions of years (Ma); MR the maximum long-term slip rate in cm/yr; D_{total} the maximum cumulative displacement in km.

Based on these four criteria, three classes of structural maturity are defined as follows (see Manighetti et al., 2007 for more details):

'Immature': $L < 300$ km, and/or I-Age < 5 Ma, and/or $MR < 1$ cm/yr, and/or $D_{total} < 10$ km.

'Intermediate': $300<L<1000$ km, and/or $5<\text{I-Age}<10$ Ma, and/or $MR \approx 1$ cm/yr, and/or D_{total} = few 10 km.

'Mature': $L > 1000$ km, and/or I-Age > 10 Ma, and/or MR = few cm/yr, and/or $D_{total} > 100$ km.

A fault needs not to have the four parameters satisfying together the above criteria for its maturity to be defined, as the criteria 'value' depends on the fault slip mode.

The slip mode of each earthquake is determined according to the classification proposed by Boore et al. (1997). Only earthquakes with $Mw \geq 6.5$ that have not broken the ground surface, are considered as blind. Others are labeled 'surface' for 'surface-breaking earthquakes'.

(1) Archuleta et al (1982); (2) Armijo et a (1999); (3) Beanland et al. (1990); (4) Berberian (1979); (5) Berry (1997); (6) Boullier et al (2004); (7) Chen et al (2001); (8) Cockerham et Corbett (1987); (9) Cotton et al. (1996); (10) Davis and Namson (1989) ; (11) Davis et Namson (1994); (12) dePolo et Ramelli (1987); (13) Doig (1998); (14) Given et al (1982); (15) Griffith et Cook (2005); (16) Hardebeck et al (2004); (17) Hauksson (1994); (18)

http://earthquake.usgs.gov/regional/qfaults/ca/index.php; (19) http://www.data.scec.org/chrono_index/quakedex.html; (20) Hubert-Ferrari et al (2002); (21) Huftile and Yeats (1996); (22) Hyndman at al. (2005); (23) Keller (1995); (24) Khattri et al. (1995); (25) Matmon et al (2006); (26) McLaren et al. (2008); (27) Miller et al (2002); (28) Murata et al (2001); (29) Nairn and Beanland (1989); (30) Nicholson (1996); (31) Petersen and Wesnousky, 1994; (32) Rockwell et al (2000); (33) Rubin et Sieh (1997); (34) Rymer et al (2002); (35) Sengor et al (2004); (36) Schaff et al (2002) ; (37) Sieh et Jahns (1984); (38) Simoes et al (2007); (39) Smith et Priestley (2000); (40) Stein et Ekstrom (1992); (41) Stirling et al (1996); (42) Talebian et Jackson (2002); (43) Tsutsumi and Yeats (1999); (45) Walker et al. (2003); (46) Wallace et al. (1981); (47) Westaway (1994); (48) Wetmiller et al. (1988); (49) Yue et al (2005).

* The Kobe earthquake was blind where the strong motions have been measured.

Table 1

EQ#	Date	Earthquake name	Country	Mw	Style of faulting	Style of rupture	Fault name	L(km)	I-Age (Ma)	D total (km)	MR (cm/an)	Maturity	References
1	09/02/1971	San Fernando	USA	6.6	Reverse	surface	Transverse Ranges fault zone: San Fernando fault	<200	6		~0.5	1	31, 43, 18
2	01/08/1975	Oroville	USA	6	Normal	-	Sierra Nevada fault system:small, secondary fault				<0.1	1	31
3	13/08/1978	Santa Barbara	USA	5.8	Reverse	-	fault	~10			0.01	1	31, 46
4	16/09/1978	Tabas	Iran	7.3	Reverse	surface	North ending of Nayband fault: Tabas fault	<100				1	4,45
5	06/08/1979	Coyote Lake	USA	5.7	Strike-slip	-	Calaveras fault	200		24	1.5 +/- 0.4	2	18, 36, 41
6	15/12/1979	Imperial Valley	USA	6.5	Strike-slip	surface	Imperial Valley fault (south part of San Jacinto fault)	> 300		24	1.5-2	2	18, 19, 31
7	25/05/1980	Mammoth Lake	USA	6.2	Normal	-	Hilton Creek fault zone	~20			~ 0.1	1	1, 5, 14
8	02/05/1983	Coalinga	USA	6.3	Reverse	-	Coalinga thrust fault	~110			0.1-0.2	1	40
9	24/04/1984	Morgan Hill	USA	6.1	Strike-slip	-	Calaveras fault	200		24	1.5 +/- 0.4	2	18, 36, 41
10	23/12/1985	Nahanni	Canada	6.7	Reverse	buried	south Mackenzie Fold Belt: English Chief Anticline	~60			<0.1	1	22, 48
11	08/07/1986	Spring	USA	6	Reverse	-	faults	~100			<0.2	1	18, 30
12	21/07/1986	Chalfant Valley	USA	6.2	Strike-slip	-	White mountain fault zone	~100			0.05-0.12	1	8, 12, 39
13	02/03/1987	Edgecumbe	USA	6.5	Normal	surface	Edgecumbe fault (Whakatane graben)	~10			0.1-0.2	1	3, 29
14	01/10/1987	Whittier Narrows	USA	5.9	Reverse	-	Transverse Ranges fault zone: Elysian park Thrust		2 - 4	10	0.17-0.53	1	10, 31
15	18/10/1989	Loma Prieta	USA	6.9	Reverse	buried	Sargent fault	<100			0.3	1	18, 31
16	28/06/1991	Sierra Madre	USA	5.6	Reverse	-	Transverse Range region, sierra madre fault zone, Clamshell-Sawpit faults	15-20			<0.1	1	15, 17, 19
17	19/10/1991	Uttarkashi	India	6.8	Reverse	buried	Main Central Thrust zone	>1000				3	9, 24
18	13/02/1992	Erzincan	Turkey	6.6	Strike-slip	surface	Central section of North Anatolian Fault	1000-1500	11-13	~100	1.5-3	3	20, 35, 47
19	28/06/1992	Landers	USA	7.3	Strike-slip	surface	Eastern California Schear zone: Johnson Valley-Emerson-Camprock fault system	<200			0.05-0.1	1	18, 19, 31, 32, 33
20	17/01/1994	Northridge	USA	6.6	Reverse	buried	Transverse Ranges fault zone :Northridge fault (eastern extension of Oak Ridge fault)	<100	2.3 - 0.5		0.1 - 0.5	1	11, 15, 18, 19, 21, 43
21	16/01/1995	Kobe	Japan	6.9	Strike-slip		Nojima fault	~10	<5		0.05-0.1	1	6, 28
22	17/08/1999	Izmit	Turkey	7.6	Strike-slip	surface	western tip of North Anatolian fault	1000-1500	~5	85	~1.5	2	2, 20, 42
23	20/09/1999	Chi-Chi	Taiwan	7.6	Reverse	surface	Chelungpu fault	100-200	0.7	~14	1.3 +/-0.5	2	7, 38, 49
24	16/10/1999	Hector Mine	USA	7.1	Strike-slip	surface	Eastern California Shear zone: Lavis Lake fault, Bullion fault	< 200			0.05-0.1	1	18, 19, 32, 33, 34
25	12/11/1999	Duzce	Turkey	7.1	Strike-slip	surface	western tip of North Anatolian fault	1000-1500	~5	85	~1.5	2	2, 20, 42
26	03/11/2002	Denali	USA	7.8	Strike-slip	surface	Denali fault system	~2000	> 30	~130	0.9-1.3	3	13, 25, 27
27	22/12/2003	San Simeon	USA	6.6	Reverse	buried	Oceanic fault or adjacent blind thrust	<100			<0.1	1	16, 23, 26
28	28/09/2004	Parkfield	USA	6	Strike-slip	-	San Andreas Fault	>1000		>150	~3	3	37, 41, 18

Figure 1

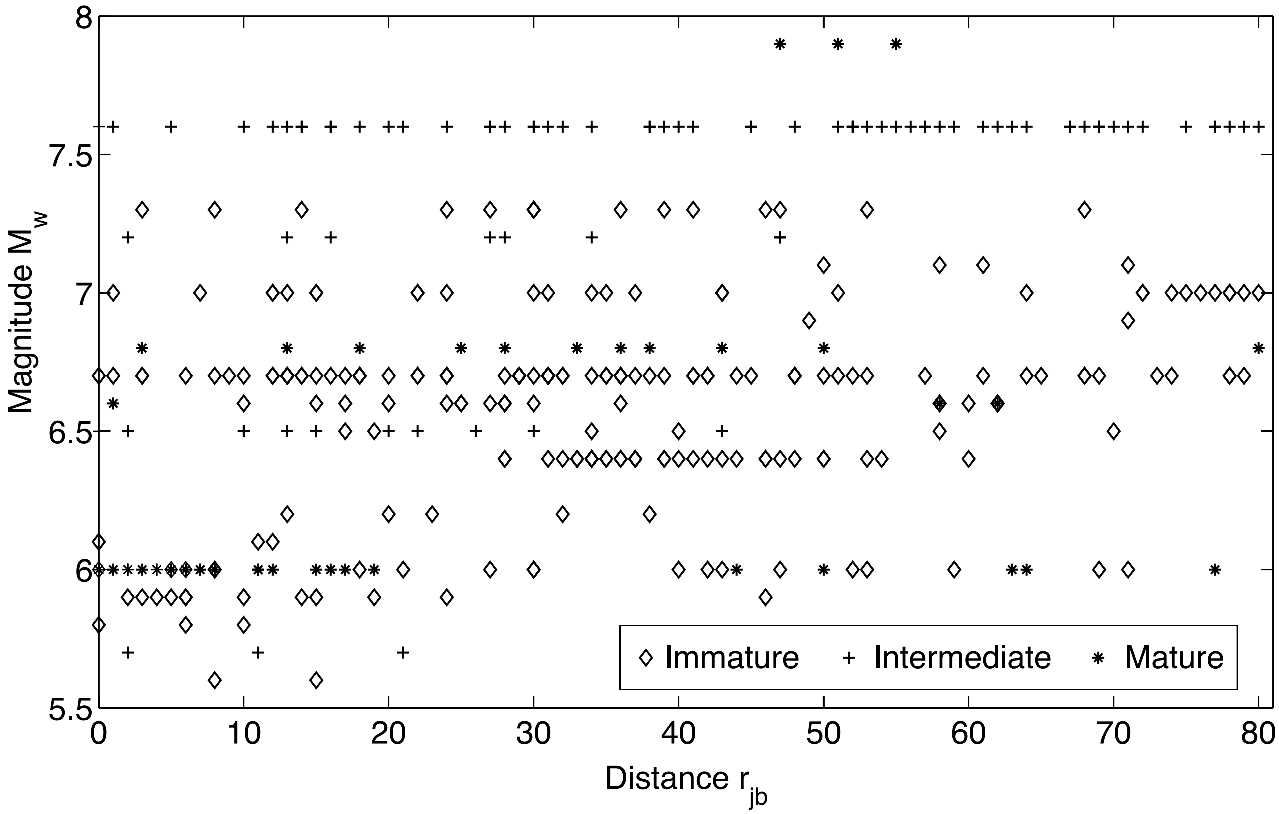

Figure 2

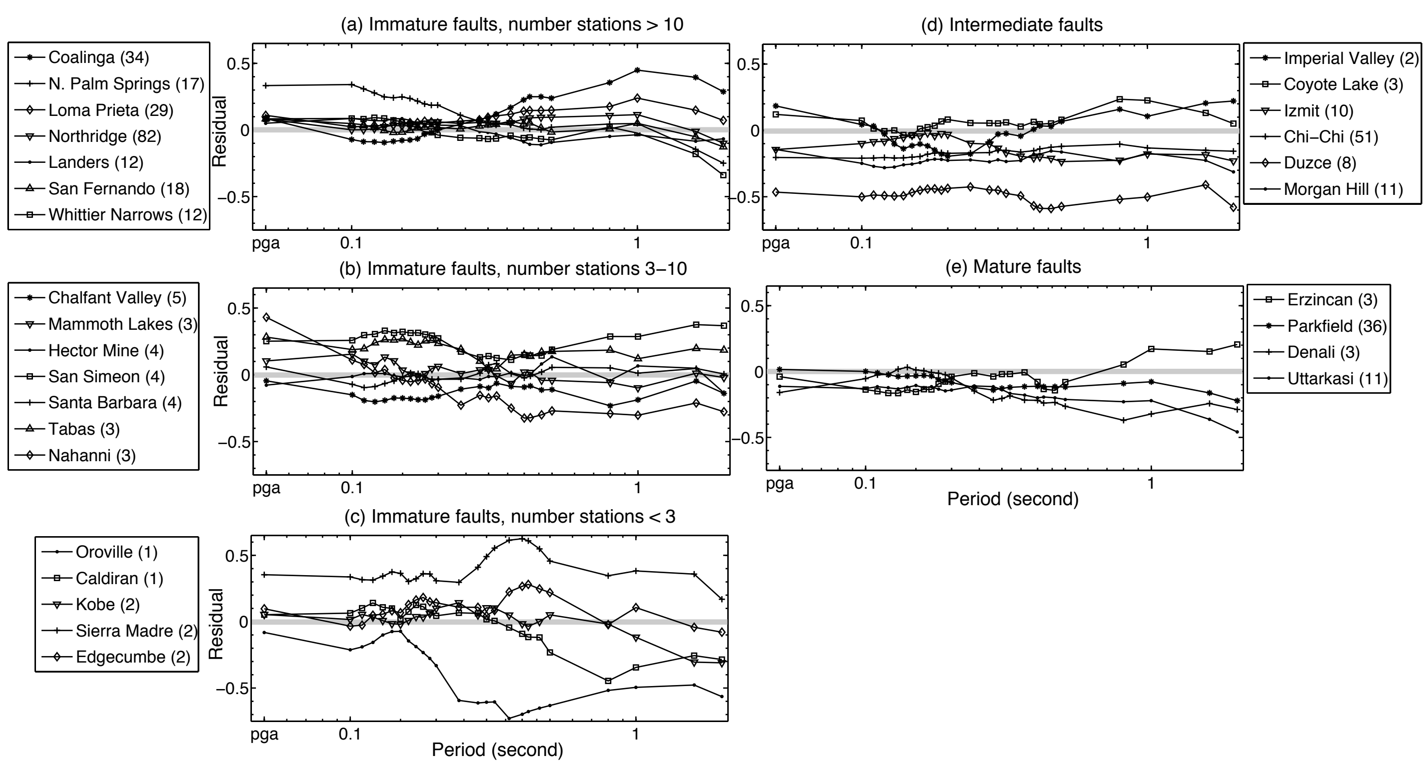

Figure 3

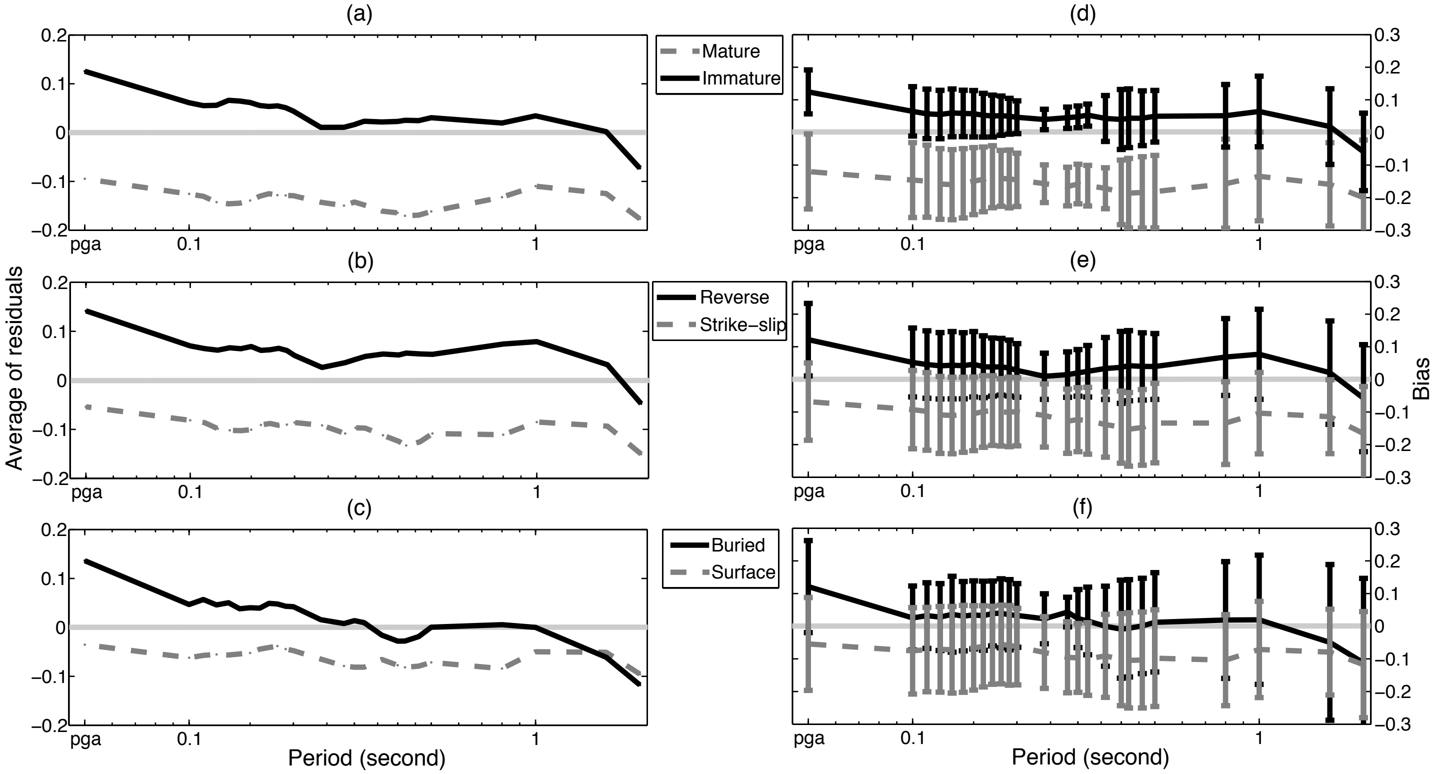

Figure 4